

Application of the Dissipative Particle Dynamics Method to Ferromagnetic Colloidal Dispersions

AKIRA SATOH

Professor, Akita Prefectural University, Japan

Roy W. Chantrell

Professor, York University, U. K.

AIChE 2006 Annual Meeting, San Francisco, California, November 12-17, 2006

ABSTRACT

We have investigated the validity of the application of the dissipative particle dynamics (DPD) method to ferromagnetic colloidal dispersions by conducting DPD simulations for a two-dimensional system. Firstly, the interaction between dissipative and magnetic particles has been idealized as some model potentials, and DPD simulations have been carried out using such model potentials for a two magnetic particle system. In these simulations, we have concentrated our attention on the collision time for the two particles approaching each other and touching from an initially separated position, and such collision time has been evaluated for various cases of the mass and diameter of dissipative particles and the model parameters, which are included in defining the equation of motion of dissipative particles. Next, we have treated a multi-particle system of magnetic particles, and have evaluated particle aggregates and the pair correlation function along an applied magnetic field direction. Such characteristics of aggregate structures have been compared with the results of Monte Carlo and Brownian dynamics simulations in order to clarify the validity of the application of the DPD method to particle dispersion systems. The present simulation results have clearly shown that DPD simulations with the model interaction potential presented here give rise to physically reasonable aggregate structures under circumstances of strong magnetic particle-particle interactions as well as a strong external magnetic field, since these aggregate structures are in good agreement with those of Monte Carlo and Brownian dynamics simulations.

1. INTRODUCTION

Computer simulation methods for solving fluid problems are mainly classified into two simulation techniques. The first one is numerical analysis methods, in which the basic equations such as the Navier-Stokes equations are discretized and such equations are numerically solved to obtain the solution of the flow field. The second one is molecular dynamics methods, in which molecules or fluid particles, that are constituents of fluids, are simulated and the solution of the flow field is obtained from the averaging procedure of microscopic velocities of molecules or fluid particles. Representative methods for the latter are lattice gas methods [1], lattice Boltzmann methods [2], dissipative particle dynamics

(DPD) methods [3-8]. In the former two methods, the fluid region is divided in a lattice formation and virtual fluid particles are allowed to move on such lattice sites. In contrast, there is not such a limitation concerning the motion of virtual particles for DPD methods. In DPD methods, clusters or groups of molecules are dealt with, and these virtual or fluid particles are simulated to obtain a flow field. In this approach, a system is regarded as being composed of such model fluid particles, and these particles interact with each other dissipatively, exchange momenta, and move randomly like Brownian particles; we call this virtual fluid particle a "dissipative particle." DPD methods are, therefore, a mesoscopic simulation technique, and we discuss the availability of DPD methods for a simulation technique of colloidal dispersions in the present study.

In molecular dynamics methods [9-11], the motion of each molecule, which constitutes a fluid, are simulated to obtain the solution of a macroscopic flow field, so that such simulations are computationally very expensive. Molecular dynamics methods, therefore, cannot be applicable to various flow problems in a wide range, but to some limited flow problems alone. In contrast, since virtual fluid particles are treated in a simulation for DPD methods, the computation time of DPD simulations can be shortened significantly compared with molecular dynamics simulations. This clearly means that DPD methods are applicable to not only pure liquid flow problems but also flow problems of suspensions composed of solid particles, in which multi-body hydrodynamic interactions among particles have significant influences on flow properties. Since multi-body hydrodynamic interactions are very difficult to be treated in simulations of a particle-liquid system, conventional simulations usually take into consideration only the friction forces between particles and the ambient fluid, instead of taking account of such multi-body interactions [12]. This tendency concerning the study by means of simulations becomes more significant for complicated suspensions or dispersions in which non-spherical particles such as rodlike ones are dispersed in a base liquid [13,14].

Some simulation techniques may be possible for solving the particle motion and the flow field simultaneously; the methods based on the Navier-Stokes equations [15-17], lattice-Boltzmann methods [18], and DPD methods [3,4,19] are representative ones. If we consider applying such simulation techniques to colloidal dispersions composed of ferromagnetic rodlike particles, of which our research group has vigorously been conducting some systematic studies [20-25], DPD methods may be regarded as the most promising simulation technique. Hence, we focus our attention on DPD methods in the present study.

The objectives of the present study are firstly to present the potential model for the interactions between dissipative and magnetic particles, and to discuss the validity of such model potentials by considering the dynamic properties for a two magnetic particle system. In concrete, the influences of model parameters [3,5,8], which are introduced in developing the equation of motion for dissipative particles, the number density, diameter, and mass of dissipative particles, on such characteristics are discussed in detail. Secondly, we consider aggregation phenomena in a many-particle system to clarify the validity of DPD methods for ferromagnetic colloidal dispersions. In concrete, the results of aggregate

structures obtained by DPD simulations are compared with those of Monte Carlo and Brownian dynamics simulations under circumstances of a strong external magnetic field.

2. DISSIPATIVE PARTICLE DYNAMICS METHODS

2.1. Kinetic equation of dissipative particles

A ferromagnetic colloidal dispersion is microscopically composed of ferromagnetic particles and molecules of a base liquid. If a base liquid is regarded as being composed of dissipative particles, the motion of magnetic particles is governed by the interactions with the other magnetic particles and ambient dissipative ones. In the following, we briefly show the kinetic equation of dissipative particles [3, 5, 8, 11].

The following three kinds of forces act on dissipative particle i : a repulsive conservative force \mathbf{F}_{ij}^C exerted by the other particles, a dissipative force \mathbf{F}_{ij}^D providing a viscous drag to the system, and a random or stochastic force \mathbf{F}_{ij}^R inducing the thermal motion of particles. The magnetic force acting on dissipative particles by magnetic ones is not taken into account in this section, since this force will be addressed in the following section. With the above-mentioned forces, the equation of motion of particle i can be written as [11]

$$m_d \frac{d\mathbf{v}_i}{dt} = \sum_{j(\neq i)} \mathbf{F}_{ij}^C + \sum_{j(\neq i)} \mathbf{F}_{ij}^D + \sum_{j(\neq i)} \mathbf{F}_{ij}^R, \quad (1)$$

in which

$$\mathbf{F}_{ij}^D = -\gamma w_D(r_{ij}) (\mathbf{e}_{ij} \cdot \mathbf{v}_{ij}) \mathbf{e}_{ij}, \quad \mathbf{F}_{ij}^R = \sigma w_R(r_{ij}) \mathbf{e}_{ij} \zeta_{ij}, \quad \mathbf{F}_{ij}^C = \alpha w_R(r_{ij}) \mathbf{e}_{ij}. \quad (2)$$

Also, m_d is the mass of particle i , \mathbf{v}_i is the velocity, and, concerning the subscripts, for example, \mathbf{F}_{ij}^C is the force acting on particle i by particle j . Also, α , γ , and σ are the constants representing the strengths of repulsive, dissipative, and random forces, respectively. The weight functions $w_D(r_{ij})$ and $w_R(r_{ij})$ are introduced such that inter-particle forces decrease with increasing particle-particle separations, and the expression for $w_R(r_{ij})$ is written as

$$w_R(r_{ij}) = \begin{cases} 1 - \frac{r_{ij}}{d_c} & \text{for } r_{ij} \leq d_c, \\ 0 & \text{for } r_{ij} > d_c. \end{cases} \quad (3)$$

The weight functions $w_D(r_{ij})$ and $w_R(r_{ij})$, and γ and σ have to satisfy the following relationships, respectively:

$$w_D(r_{ij}) = w_R^2(r_{ij}), \quad \sigma^2 = 2\gamma kT. \quad (4)$$

In the above equations, d_c is the apparent diameter of dissipative particles, \mathbf{r}_{ij} is the relative position ($r_{ij} = |\mathbf{r}_{ij}|$), given by $\mathbf{r}_{ij} = \mathbf{r}_i - \mathbf{r}_j$, \mathbf{e}_{ij} is the unit vector denoting the direction of particle i relative to particle j , expressed as $\mathbf{e}_{ij} = \mathbf{r}_{ij}/r_{ij}$, \mathbf{v}_{ij} is the relative velocity, expressed as $\mathbf{v}_{ij} = \mathbf{v}_i - \mathbf{v}_j$,

k is Boltzmann's constant, and T is the liquid temperature. Also, ζ_{ij} is a random variable inducing the random motion of particles.

If Eq. (1) is integrated with respect to time over a small time interval from t to $t+\Delta t$, then the finite difference equations governing the particle motion in simulations can be obtained as

$$\Delta \mathbf{r}_i = \mathbf{v}_i \Delta t, \quad (5)$$

$$\Delta \mathbf{v}_i = \frac{\alpha}{m_d} \sum_{j(\neq i)} w_R(r_{ij}) \mathbf{e}_{ij} \Delta t - \frac{\gamma}{m_d} \sum_{j(\neq i)} w_R^2(r_{ij}) (\mathbf{e}_{ij} \cdot \mathbf{v}_{ij}) \mathbf{e}_{ij} \Delta t + \frac{(2\gamma kT)^{1/2}}{m_d} \sum_{j(\neq i)} w_R(r_{ij}) \mathbf{e}_{ij} \theta_{ij} \sqrt{\Delta t}, \quad (6)$$

in which θ_{ij} is the stochastic variable and has to satisfy the following stochastic properties:

$$\langle \theta_{ij} \rangle = 0, \quad \langle \theta_{ij} \theta_{i'j'} \rangle = (\delta_{ii'} \delta_{jj'} + \delta_{ij'} \delta_{ji'}), \quad (7)$$

in which δ_{ij} is the Kronecker delta. In simulations, the stochastic variable θ_{ij} is sampled from a uniform or normal distribution with zero average value and unit variance [3-5].

2.2. Kinetic equation of magnetic particles

A magnetic particle is idealized as a spherical particle with a central point dipole coated with a uniform surfactant layer (or a steric layer). If the diameter of the solid part of such particles, the thickness of the steric layer, and the diameter including the steric layer, are denoted by d_s , δ , and $d (= d_s + 2\delta)$, respectively, then the magnetic interaction energy between particles i and j , $u_{ij}^{(m)}$, and the particle-field interaction energy, $u_i^{(H)}$, and the interaction energy arising due to the overlapping of the steric layers, $u_{ij}^{(V)}$, are expressed, respectively, as [11]

$$u_{ij}^{(m)} = \frac{\mu_0}{4\pi r_{ij}^3} \{ \mathbf{m}_i \cdot \mathbf{m}_j - 3(\mathbf{m}_i \cdot \mathbf{t}_{ij})(\mathbf{m}_j \cdot \mathbf{t}_{ij}) \}, \quad (8)$$

$$u_i^{(H)} = -\mu_0 \mathbf{m}_i \cdot \mathbf{H}, \quad (9)$$

$$u_{ij}^{(V)} = kT\lambda_V \left\{ 2 - \frac{2r_{ij}/d_s}{t_\delta} \ln \left(\frac{d}{r_{ij}} \right) - 2 \frac{r_{ij}/d_s - 1}{t_\delta} \right\}, \quad (10)$$

in which μ_0 is the permeability of free space, \mathbf{m}_i is the magnetic moment ($m_0 = |\mathbf{m}_i|$), \mathbf{t}_{ij} is the unit vector given by \mathbf{r}_{ij}/r_{ij} , $\mathbf{r}_{ij} = \mathbf{r}_i - \mathbf{r}_j$, $r_{ij} = |\mathbf{r}_{ij}|$, \mathbf{H} is the applied magnetic field ($H = |\mathbf{H}|$), and t_δ is the ratio of the thickness of steric layer δ to the radius of the solid part of the particle, equal to $2\delta/d_s$. The nondimensional parameter λ_V , appearing in Eq. (10), represents the strength of steric particle-particle interactions relative to the thermal energy, expressed as $\lambda_V = \pi d_s^2 n_s / 2$, in which n_s is the number of surfactant molecules per unit area on the particle surface.

From Eqs. (8) and (10), the forces acting on particle i are written as

$$\mathbf{F}_{ij}^{(m)} = -\frac{3\mu_0}{4\pi r_{ij}} \left[-(\mathbf{m}_i \cdot \mathbf{m}_j) \mathbf{t}_{ij} + 5(\mathbf{m}_i \cdot \mathbf{t}_{ij})(\mathbf{m}_j \cdot \mathbf{t}_{ij}) \mathbf{t}_{ij} - \{(\mathbf{m}_j \cdot \mathbf{t}_{ij}) \mathbf{m}_i + (\mathbf{m}_i \cdot \mathbf{t}_{ij}) \mathbf{m}_j\} \right], \quad (11)$$

$$\mathbf{F}_{ij}^{(V)} = \frac{kt\lambda_V}{\delta} \cdot \frac{\mathbf{r}_{ij}}{r_{ij}} \ln\left(\frac{d}{r_{ij}}\right) \quad (d_s \leq r_{ij} \leq d). \quad (12)$$

Besides these forces, the forces by dissipative particles have to be taken into account, but are not treated here, since they will be addressed in the following section.

The motion of magnetic particles are specified by Newton's equations, so that such equations are discretized concerning time to obtain the finite difference equations governing the particle motion in simulations:

$$\Delta \mathbf{r}_i = \mathbf{v}_i \Delta t, \quad (13)$$

$$\Delta \mathbf{v}_i = \sum_{j(\neq i)} \mathbf{F}_{ij} \Delta t / m_m, \quad (14)$$

in which m_m is the mass of magnetic particles and $\mathbf{F}_{ij} = \mathbf{F}_{ij}^{(m)} + \mathbf{F}_{ij}^{(V)}$.

2.3. Model potential for interactions between dissipative and magnetic particles

In the previous example of the application of DPD methods to colloidal dispersions [3, 4, 19], each colloidal particle is modeled as a group of dissipative particles. In this case, the interactions of the magnetic particle of interest with the ambient dissipative particles are treated as the interactions between ambient dissipative particles and the constituent dissipative ones of the magnetic particle. However, the interactions between colloidal particles and solvent molecules in a real dispersion ought to depend on the characteristics of the dispersion of interest. In other words, such interactions are strongly dependent on the mass and diameter ratios of colloidal particles to solvent molecules, the properties of the interaction potential between such particles, etc. If we take into account that dissipative particles themselves are just a virtual particle which is a cluster or group of solvent molecules, it may be possible to use a model potential for the interaction between dissipative and magnetic particles, instead of regarding a colloidal particle as a group of dissipative particles.

The most simple potential model may be the hard sphere potential, in which magnetic particles are regarded as a hard sphere and dissipative particles are elastically reflected at the contact with a magnetic particle. Another simple potential model may be the Lennard-Jones potential. Although the present study adopts the latter model potential and attempts to discuss its validity, the simple form of the Lennard-Jones potential based on each center of dissipative and magnetic particles causes an extraordinary overlap between such particles. Hence, as shown in Fig. 1, we consider a inscribed sphere with the same diameter of dissipative particles, which is located on the line connected between each center of dissipative and magnetic particles, and apply the Lennard-Jones potential to such an inscribed particle and dissipative particles. That is, the interaction energy u_{ip} for

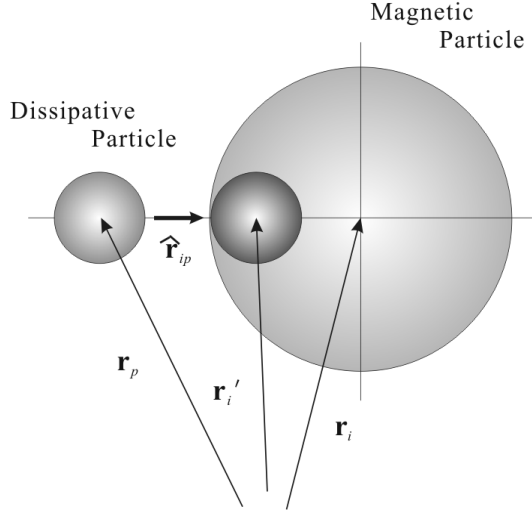


FIG.1. Model of interaction between magnetic and dissipative particles.

dissipative particle p and magnetic particle i is expressed as

$$u_{ip} = 4\varepsilon \left\{ \left(\frac{d_c}{r'_{ip}} \right)^m - \left(\frac{d_c}{r'_{ip}} \right)^n \right\}, \quad (15)$$

in which ε is the constant representing the strength of such an interaction, $\mathbf{r}'_{ip} = \mathbf{r}'_i - \mathbf{r}_p$, $r'_{ip} = |\mathbf{r}'_{ip}|$, \mathbf{r}_i is the position vector of the center of magnetic particle, \mathbf{r}_p is the similar position vector of dissipative particle p , and \mathbf{r}'_i is that of the above-mentioned inscribed sphere. The expression for \mathbf{r}'_i is written as

$$\mathbf{r}'_i = \mathbf{r}_i - (d - d_c/2) \hat{\mathbf{r}}_{ip}, \quad (16)$$

in which $\hat{\mathbf{r}}_{ip} = \mathbf{r}_{ip}/r_{ip}$, $\mathbf{r}_{ip} = \mathbf{r}_i - \mathbf{r}_p$, and $r_{ip} = |\mathbf{r}_{ip}|$. If we set $m=12$ and $n=6$ in Eq. (15), the model potential leads to the famous Lennard-Jones 12-6 potential. In the present study, we discuss several cases of the model potentials with $(m, n) = (12, 6)$, $(8, 4)$, etc.

From the expression of the interaction energy in Eq. (15), the force acting on dissipative particle p by magnetic particle i , $\mathbf{F}_{ip}^{(int)}$, is expressed as

$$\mathbf{F}_{ip}^{(int)} = 4n\varepsilon \left\{ \frac{m}{n} \left(\frac{d_c}{r'_{ip}} \right)^m - \left(\frac{d_c}{r'_{ip}} \right)^n \right\} \frac{\hat{\mathbf{r}}_{ip}}{r'_{ip}}. \quad (17)$$

2.4. Non-dimensionalization of the equation of motion and related quantities

To non-dimensionalize each quantity, the following representative values are used: d for distances, m_m for masses, kT for energies, $(kT/m_m)^{1/2}$ for velocities, $d(m_m/kT)^{1/2}$ for time,

kT/d for forces, etc. With these representative values, Eqs. (5) and (6) can be non-dimensionalized as

$$\Delta \mathbf{r}_i^* = \mathbf{v}_i^* \Delta t^*, \quad (18)$$

$$\begin{aligned} \Delta \mathbf{v}_i^* = & \frac{1}{m_d^* d_c^*} \alpha^* \sum_{j(\neq i)} w_R(r_{ij}^*) \mathbf{e}_{ij} \Delta t^* - \frac{1}{(m_d^*)^{1/2} d_c^*} \gamma^* \sum_{j(\neq i)} w_R^2(r_{ij}^*) (\mathbf{e}_{ij} \cdot \mathbf{v}_{ij}^*) \\ & \times \mathbf{e}_{ij} \Delta t^* + \frac{1}{(m_d^*)^{3/4} d_c^{*1/2}} (2\gamma^*)^{1/2} \sum_{j(\neq i)} w_R(r_{ij}^*) \mathbf{e}_{ij} \theta_{ij} \sqrt{\Delta t^*} - \frac{1}{m_d^*} \sum_k \mathbf{F}_{ki}^{(int)*} \Delta t^*, \end{aligned} \quad (19)$$

in which

$$w_R(r_{ij}^*) = \begin{cases} 1 - r_{ij}^*/d_c^* & \text{for } r_{ij}^*/d_c^* \leq 1, \\ 0 & \text{for } r_{ij}^*/d_c^* > 1, \end{cases} \quad (20)$$

$$\alpha^* = \alpha \frac{d_c}{kT}, \quad \gamma^* = \gamma \frac{d_c}{(m_d kT)^{1/2}}. \quad (21)$$

In the above equations, the superscript * means non-dimensionalized quantities. It is noted that Eq. (19) includes the forces due to the interactions with magnetic particles, described in Sec. 2.3.

Similarly, the non-dimensional form of Eqs. (13), (14), (11), and (12) are expressed as

$$\Delta \mathbf{r}_i^* = \mathbf{v}_i^* \Delta t^*, \quad (22)$$

$$\Delta \mathbf{v}_i^* = \sum_{j(\neq i)} \mathbf{F}_{ij}^* \Delta t^* + \sum_p \mathbf{F}_{ip}^{(int)*} \Delta t^*, \quad (23)$$

$$\mathbf{F}_{ij}^{(m)*} = -3\lambda \frac{1}{t_{ij}^{4*}} \left[-(\mathbf{n}_i \cdot \mathbf{n}_j) \mathbf{t}_{ij} + 5(\mathbf{n}_i \cdot \mathbf{t}_{ij})(\mathbf{n}_j \cdot \mathbf{t}_{ij}) \mathbf{t}_{ij} - \{(\mathbf{n}_j \cdot \mathbf{t}_{ij}) \mathbf{n}_i + (\mathbf{n}_i \cdot \mathbf{t}_{ij}) \mathbf{n}_j\} \right], \quad (24)$$

$$\mathbf{F}_{ij}^{(V)*} = \lambda_V \frac{1}{t_{ij}^*} \ln \left(\frac{1}{r_{ij}^*} \right) \quad (d_s^* \leq r_{ij}^* \leq 1), \quad (25)$$

in which $\mathbf{F}_{ij}^* = \mathbf{F}_{ij}^{(m)*} + \mathbf{F}_{ij}^{(V)*}$, \mathbf{n}_i is the unit vector denoting the direction of the magnetic moment \mathbf{m}_i , expressed as $\mathbf{n}_i = \mathbf{m}_i / m_0$ ($m_0 = |\mathbf{m}_i|$). The non-dimensional parameter λ in Eq. (24) means the strength of magnetic particle interactions relative to the thermal energy, expressed as $\lambda = \mu_0 m_0^2 / 4\pi d^3 kT$. A slightly different parameter $\lambda_s = (d/d_s)^3 \lambda$ ($= \mu_0 m_0^2 / 4\pi d_s^3$), which is defined based on the diameter of the solid part, may be useful in order to compare the present results with the previous ones obtained by Monte Carlo and Brownian dynamics simulations.

The expression of the force between dissipative and magnetic particles is written in a non-dimensional form as

$$\mathbf{F}_{ip}^* = \lambda_\epsilon \left\{ \frac{m}{n} \left(\frac{d_c^*}{r_{ip}^*} \right)^m - \left(\frac{d_c^*}{r_{ip}^*} \right)^n \right\} \frac{\hat{\mathbf{r}}_{ip}}{r_{ip}^*/d_c^*}, \quad (26)$$

in which λ_ϵ is the non-dimensional parameter representing the strength of the interaction, expressed as $\lambda_\epsilon = 4n\epsilon/(kTd_c^*)$.

In the present study, we consider a two-dimensional system in thermodynamic equilibrium, so that the relationship between the system temperature and the mean kinetic energy of one dissipative particle is expressed from the equi-partition law of energies as

$$\overline{\frac{1}{2}m_d v_d^2} = 2 \frac{kT}{2}. \quad (27)$$

From this equation, the mean square velocity of dissipative particles, $\overline{v_d^{*2}}$, is written as

$$\overline{v_d^{*2}} = \frac{2}{m_d^*}. \quad (28)$$

Similarly, the mean square velocity of magnetic particles, $\overline{v_m^{*2}}$, is expressed as

$$\overline{v_m^{*2}} = 2. \quad (29)$$

The number density of dissipative particles is non-dimensionalized as

$$n_d^* = n_d d^2 = n_d d_c^2 (d/d_c)^2 = \hat{n}_d^* / d_c^{*2}. \quad (30)$$

Instead of n_d^* , the non-dimensional density \hat{n}_d^* based on the diameter of dissipative particles may be useful for grasping the packing situation of dissipative particle directly. The non-dimensional number density of magnetic particles is expressed as $n_m^* = n_m d^2$.

3. PARAMETERS FOR SIMULATIONS

In the present study, we consider a two-dimensional dispersion composed of ferromagnetic particles to investigate the validity of the application of the DPD method to such a system. The equation of motion of dissipative particles includes many indefinite factors such as the particle diameter, mass, and various model parameters, so that we concentrate our attention on a simplified case that an external magnetic field is strong enough to neglect the rotational motion of magnetic particles; in this situation, each magnetic moment always points to the magnetic field direction. Firstly, we treat a two magnetic particle system to discuss the collision time for the two particles approaching each other and touching from an initially separated position. Such collision time is evaluated for several cases of the above-mentioned model potentials and for various cases of the mass and diameter of dissipative particles and the model parameters. Next, we treat a multi-particle system composed of eighty-one magnetic particles to evaluate particle

aggregates and the pair correlation function along the applied magnetic field direction. These results are compared with those obtained by Brownian dynamics and Monte Carlo simulations in order to clarify the validity of the application of the DPD method to particle dispersion systems.

For a two-particle system, simulations have been conducted for four cases of the model potential in Eq. (15) such as $(m,n)=(12,6)$, $(8,4)$, $(4,2)$, and $(2,1)$. For the case of simulations for multi-particle systems, we have concentrated our attention on one specific model potential of $(m,n)=(12,6)$. Representative parameters used for the present simulations are $\gamma^*=10$, $\alpha^*=\gamma^*/10$, $m_d^*=0.01$, $d_c^*=0.4$, $\lambda_e=10$, $\hat{n}_d^*=1$, and $\Delta t^*=0.0001$. Equation (19) shows that the distance of the movement of dissipative particles per unit time step becomes longer with decreased values of m_d^* and d_c^* . Thus, the time interval Δt^* has been adjusted in proportion to the product of m_d^* and d_c^* . That is, a smaller value of the time interval has been used for a decreased value of $m_d^*d_c^*$. The total number of simulation steps, $N_{time\text{max}}$, was sufficient when the condition of $\Delta t^*N_{time\text{max}}=100$ was satisfied.

4. RESULTS AND DISCUSSION

4.1. Influence of model potentials and model parameters on dynamic properties of magnetic particles for a two magnetic particle system

We have evaluated the contact time t_{cont} for two magnetic particles touching each other from an initially separated position; the magnetic particles are initially located along the magnetic field direction with the separation of $1.8d$ in the square summation region with the side length $4d$. The results of t_{cont} , which will be shown later, were obtained by averaging the data, which were evaluated for ten different cases of uniform random number sequences; random numbers are necessary for generating the random motion of dissipative particles. Unless specifically noted, the results were obtained for the representative case of $\hat{n}_d^*=1$, $\lambda_s=20$, $\lambda_e=10$, $\gamma^*=10$, $\alpha^*=\gamma^*/10$, $m_d^*=0.01$, and $d_c^*=0.4$.

Figure 2 shows the influence of λ_e on the non-dimensional contact time t_{cont}^* for four cases of the model potential in Eq. (15), i.e., for $(m,n)=(12,6)$, $(8,4)$, $(4,2)$, and $(2,1)$. It is seen that, since magnetic particles do the Brownian motion due to the interactions with the ambient dissipative particles, the qualitative features are difficult to be grasped clearly, especially for $(m,n)=(4,2)$ and $(2,1)$. However, an almost satisfactory agreement of the results is obtained for the cases of $(m,n)=(12,6)$ and $(8,4)$ within the range over $\lambda_e=10$. Hence, we concentrate our attention on the case of $(m,n)=(12,6)$ with $\lambda_e=10$ for discussing the influences of the other factors in the following.

Figure 3 shows the influence of γ^* on the contact time t_{cont}^* , in which α^* is taken as $\alpha^*=\gamma^*/10$. It is seen that the value of t_{cont}^* increases with values of γ^* , that is, longer time is necessary for two particles touching each other for larger values of γ^* . The previous results [8] have shown that the viscosity due to dissipative forces becomes large with increased

values of γ^* , which means that magnetic particles feel larger resistance in moving among the ambient dissipative particles for such cases. Hence, the qualitative features in Fig. 3 may be quite physically reasonable.

Figure 4 shows the influence of the mass of dissipative particles, m_d^* , on the contact time t_{cont}^* . It is seen from this figure that the contact time becomes longer as the value of m_d^* increases. That the mass of dissipative particles is large means that dissipative particles move more slowly for the larger mass when magnetic particles bump with the surrounding dissipative particles. Hence, it is quite understandable that magnetic particles take longer time for larger values of the mass, shown in Fig. 4.

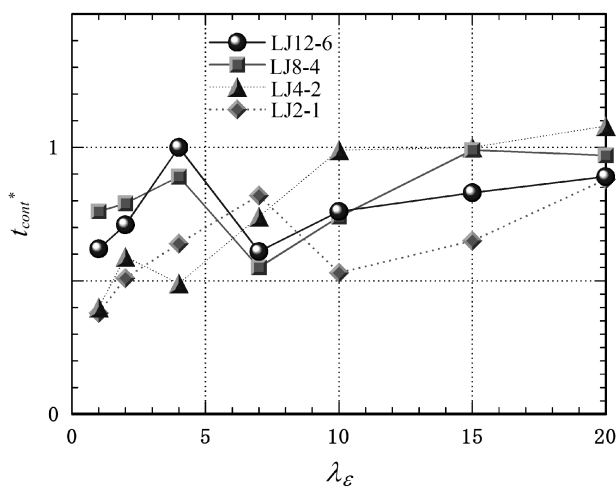


FIG.2. Dependence of collision time t_{cont}^* on interaction parameter λ_ϵ .

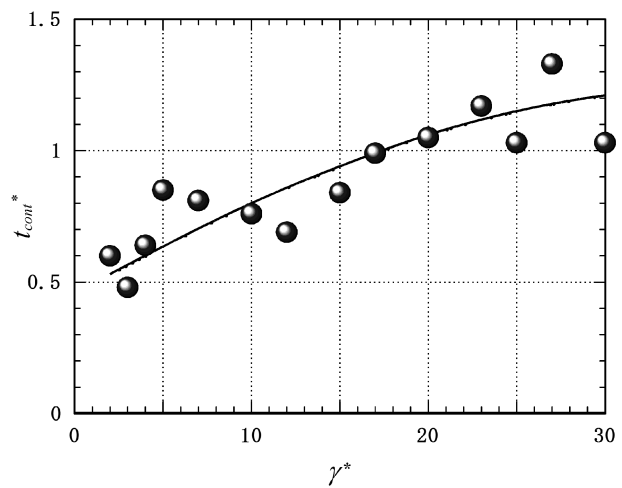


FIG.3. Dependence of collision time t_{cont}^* on dissipative force parameter γ^* .

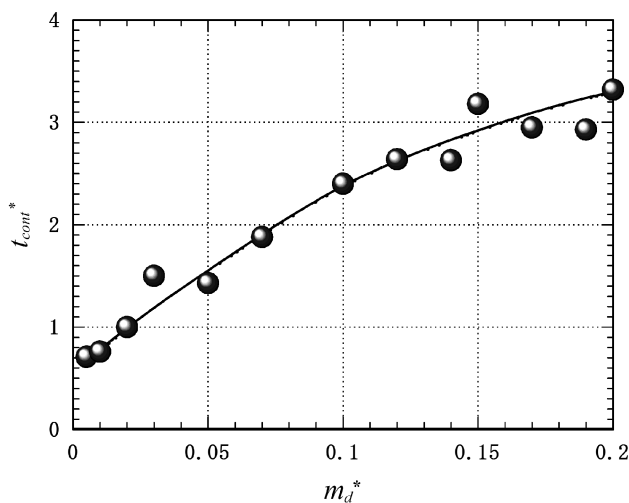


FIG.4. Dependence of collision time t_{cont}^* on particle mass m_d^* .

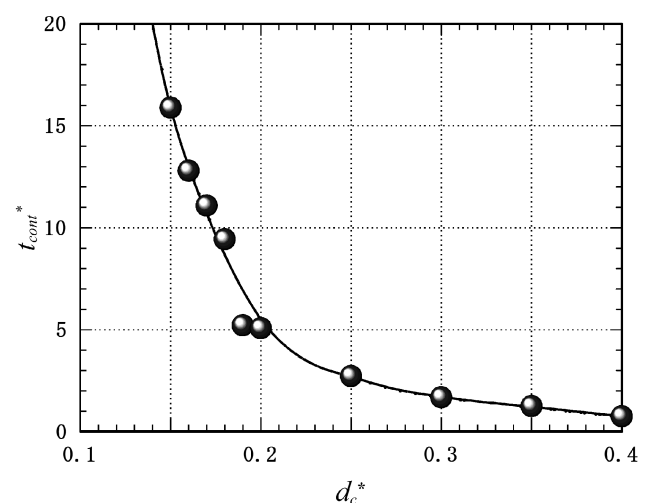


FIG.5. Dependence of collision time t_{cont}^* on particle diameter d_c^* .

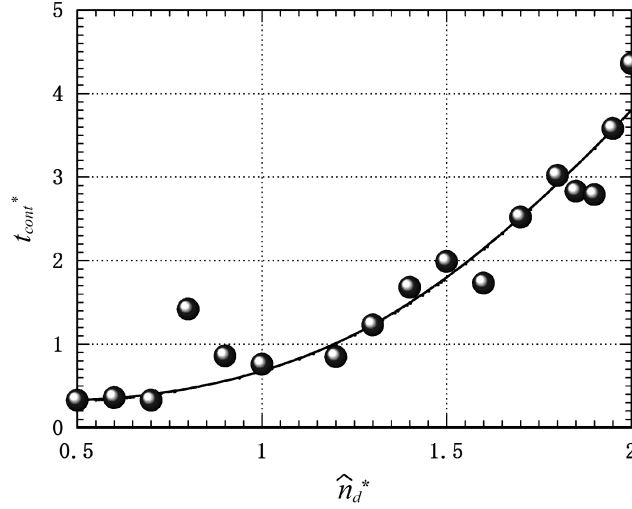


FIG.6. Dependence of collision time t_{cont}^* on particle number density \hat{n}_d^* .

Figure 5 shows the influence of the diameter of dissipative particles, d_c^* , on the contact time t_{cont}^* . We see from this figure that the contact time becomes shorter with increased values of the diameter. Since the mass of dissipative particles remains constant such as $m_d^*=0.01$, the density of dissipative particles becomes smaller with increasing the diameter, and the ambient dissipative particles around magnetic ones becomes fewer. Hence, magnetic particles can move more easily among dissipative particles in such cases, which leads to shorter contact time.

Figure 6 shows the influence of the number density of dissipative particles, \hat{n}_d^* , on the contact time t_{cont}^* . It is seen from Fig. 6 that the contact time becomes longer as the number density increases. That the number density of dissipative particles is large means that the viscosity of the base liquid is large from a macroscopic point of view, and also that, from a microscopic point of view, there are many dissipative particles, obstructing the motion of magnetic particles, around them. Hence, it is quite physically reasonable that the contact time becomes longer with increasing the number density of dissipative particles.

4.2. Validity of aggregate structures for a many magnetic particle system

4.2.1. Influence of mass of dissipative particles on aggregate structures

We treat a multi-particle system with the number density of $n_m^* \approx 0.4$, composed of eighty-one magnetic particles, to investigate the influence of the mass of dissipative particles on aggregate structures of magnetic particles. Figure 7 shows the results of aggregate structures in thermodynamic equilibrium for two cases of magnetic particle-particle interactions, i.e., for $\lambda_s=10$ and 3. Unless specifically noted, all simulation results were obtained under circumstances of $d_c^*=0.4$ and other representative values of parameters, which have already been shown in Sec. 4.1. Figures 7(a) and 7(b) are for the

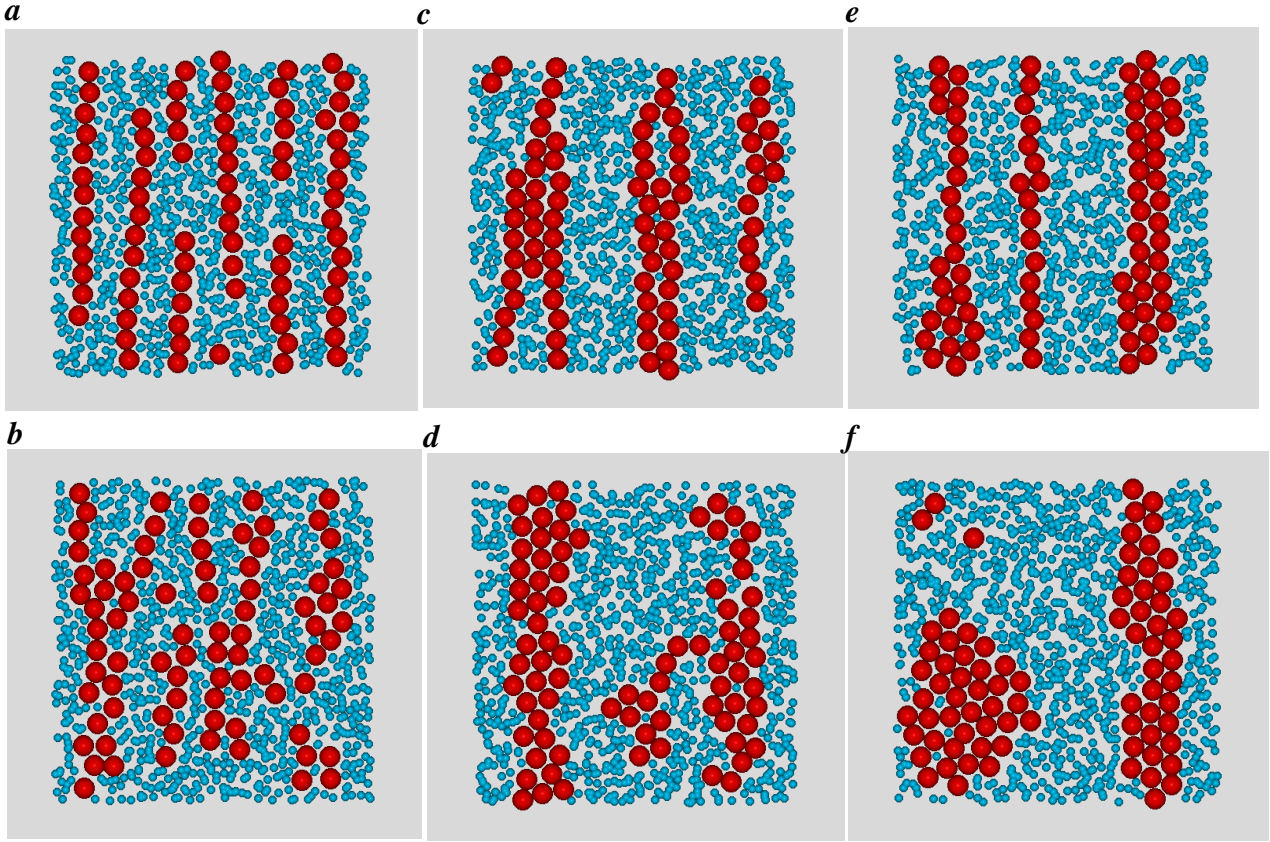


FIG.7. Influence of particle mass m_d^* on aggregate structures for $d_c^* = 0.4$: (a) for $m_d^* = 0.05$ and $\lambda_s^* = 10$, (b) for $m_d^* = 0.05$ and $\lambda_s^* = 3$, (c) for $m_d^* = 0.01$ and $\lambda_s^* = 10$, (d) for $m_d^* = 0.01$ and $\lambda_s^* = 3$, (e) for $m_d^* = 0.005$ and $\lambda_s^* = 10$, and (f) for $m_d^* = 0.005$ and $\lambda_s^* = 3$.

mass of dissipative particles, $m_d^* = 0.05$, Figs. 7(c) and (d) for $m_d^* = 0.01$, and Figs. 7(e) and 7(f) for $m_d^* = 0.005$; Figs. 7(a), 7(c) and 7(e) were obtained for $\lambda_s = 10$, and Figs. 7(b), 7(d) and 7(f) were for $\lambda_s = 3$. In the figures, small and large circles are dissipative and magnetic particles, respectively. We here concentrate our attention on the influences of the model parameters on particle aggregate structures, and the validity of aggregate structures themselves, therefore, will be discussed in the later section by comparing the present results with those obtained by Monte Carlo and Brownian dynamics simulations.

Since magnetic particle-particle interactions are much more dominant than the thermal energy for $\lambda_s = 10$, magnetic particles aggregate to form chain-like clusters along the magnetic field direction, which was clearly shown in the previous works [26]. It is seen from Figs. 7(a), (c) and (e) that the present DPD simulation results also reproduce such cluster formation qualitatively well. However, aggregate structures in Figs 7(a), (c) and (e) seem to be strongly dependent on the mass of dissipative particles. That is, although only thin chain-like clusters are formed for the case of a relatively large mass such as $m_d^* = 0.05$, magnetic particles come to form thicker chain-like clusters with decreasing values of the particle mass. Now, we have to consider why much thicker chain-like clusters tend to be formed with decreasing the mass of dissipative particles. If the mass of dissipative particles

is small, magnetic particles ought to move easily by separating the ambient particles away to approach each other. The thin chain-like clusters shown in Fig. 7(a), therefore, have a sufficient probability to aggregate to form thicker chain-like clusters such as those shown in Fig. 7(e). On the other hand, it is seen from Eq. (28) that dissipative particles with a smaller mass move with a larger average velocity for a given system temperature. Hence, although chain-like cluster can grow thick to a certain degree, and, after that, the Brownian motion of magnetic particles due to such active motion of dissipative particles disturbs a furthermore growing of thick chain-like clusters.

Since magnetic particle-particle interactions are of the slightly larger order of the thermal energy for $\lambda_s=3$, significant aggregates should not be formed for this case. However, the present DPD simulations exhibit significant cluster formation with decreasing the mass of dissipative particles; such false aggregate formation is significant for $m_d^*=0.005$, and also relatively long chain-like clusters are formed even for $m_d^*=0.05$. Two reasons may be possible for these physically unreasonable aggregate formation. Firstly, the present stimulations do not take into consideration the rotational motion of magnetic particles. Under real situations such as a limited magnetic field strength, the direction of the magnetic moment of particles is less restricted to the magnetic field direction with decreasing the magnetic properties of particles. In other words, magnetic particles do the rotational Brownian motion in such situations, which makes it difficult for magnetic particles to aggregate along the magnetic field direction. Hence, the first possible reason is that we do not use the equation of motion which can simulate the rotational motion of magnetic particles, besides the transnational motion. The model potential, employed here for interactions between magnetic and dissipative particles, may be regarded as the second possible reason. As already pointed out in Sec. 2.3, the force of a dissipative particle acts on a magnetic particle along the line between each center of these particles, which means that the rotational motion of the magnetic particle is not induced by the forces due to dissipative particles. The above two possible reasons may explain the features of unreasonable aggregate structures shown in Fig. 7. For the case of Fig. 7(f), some large pack of aggregate structures are formed even for $\lambda_s=3$, which are induced by the ambient dissipative particles that actively move around magnetic particles. The outer magnetic particles of these clusters are forced in the direction of the center of the clusters by the ambient dissipative particles, so that such large particles remain in such a form without being divided into small clusters. The thick chain-like clusters along the field direction in Fig. 7(f) is not physically reasonable, as pointed out previously, and these aggregate structures are formed too exaggeratedly due to the present simplified equation of motion without the particle rotational motion; since magnetic particle-particle interactions are slightly larger than the thermal energy for $\xi_s=3$, only short clusters ought to be formed at most under such circumstances.

Finally, we consider what the appropriate mass of dissipative particles is for obtaining physically reasonable results. As already pointed out previously, dissipative particles are virtual and regarded as groups or clusters of really solvent molecules, so that it seems to be reasonable for the mass density of dissipative particles to be taken as roughly equal to the mass density of the base liquid of a dispersion system, which one considers for

evaluating physical quantities experimentally. In the present study, we treat a ferromagnetic colloidal dispersion in which metallic ferromagnetic fine particles are assumed to be dispersed into a base liquid such as kerosene or water. In this case, if the ratio of the mass density of magnetic particles to dissipative ones is regarded as 5~8, then the ratio of mass is 0.013~0.008 for $d_c^*=0.4$, and 0.0016~0.001 for $d_c^*=0.2$. Hence, it is for the case of $d_c^*=0.4$ and $m_d^*=0.01$ that physically reasonable aggregate structures can be regarded as being reproduced. This consideration will be verified later by comparing with the results obtained by Monte Carlo and Brownian dynamics simulations.

4.2.2. Comparison with results obtained by Brownian dynamics and Monte Carlo simulations

In order to verify the validity of the DPD simulation method, we compare the present results with those which were obtained by other simulation methods. Figures 8(a) and 8(b) show the results obtained by the cluster-moving Monte Carlo method [11, 26], Figs. 8(c) and 8(d) by the Brownian dynamics method [27], and Figs. 8(e) and 8(f) by the Stokesian dynamics method [28]. Each figure has snapshots for two cases of $\lambda_s=10$ and 3. It is

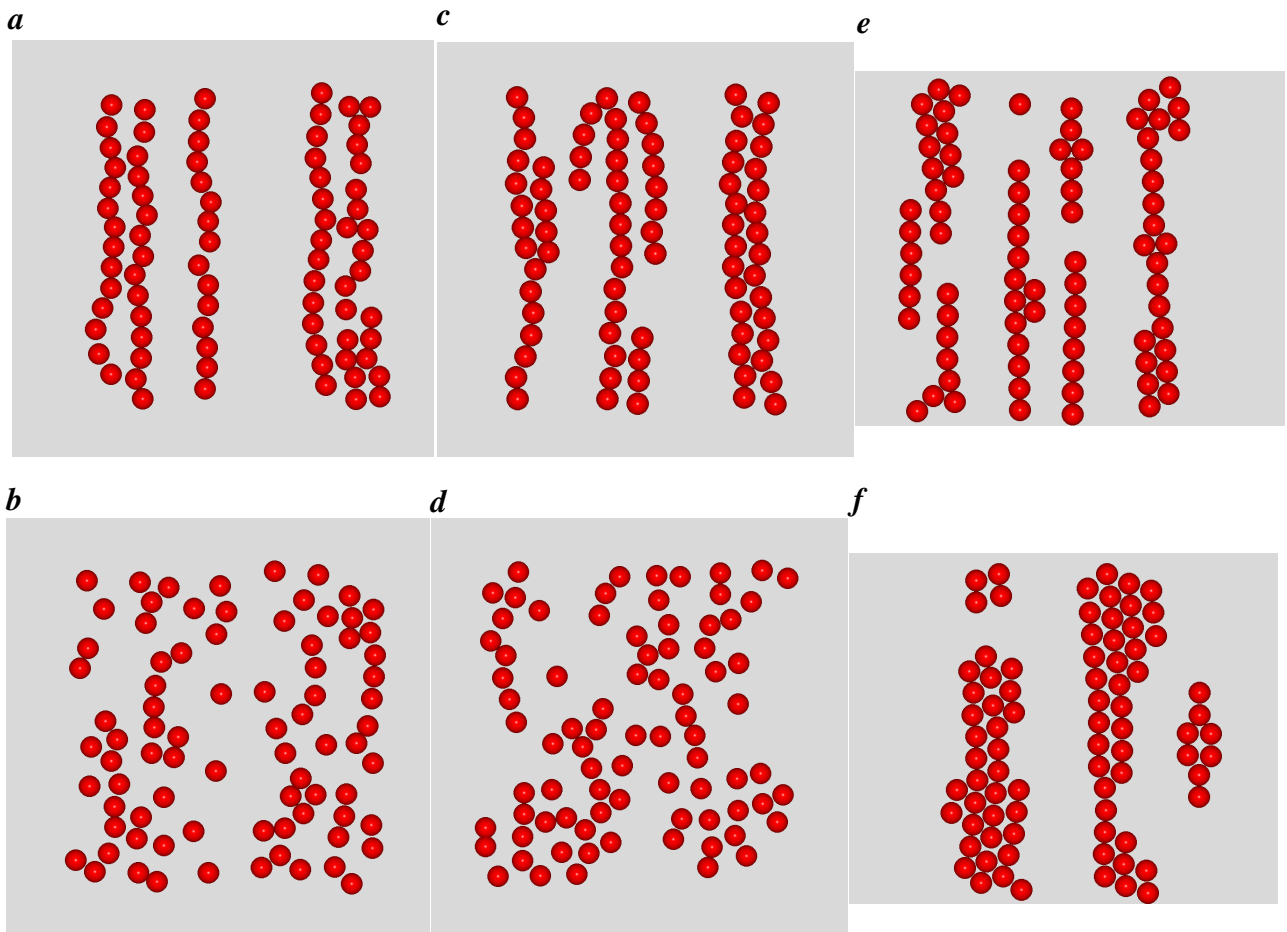


FIG.8. Aggregate structures obtained by other simulation methods for $\lambda_s^* = 10$ and 3: (a) for $\lambda_s^* = 10$ and (b) for $\lambda_s^* = 3$ by Monte Carlo simulations; (c) for $\lambda_s^* = 10$ and (d) for $\lambda_s^* = 3$ by Brownian dynamics simulations; (e) for $\lambda_s^* = 10$ and (f) for $\lambda_s^* = 3$ by Stokesian dynamics.

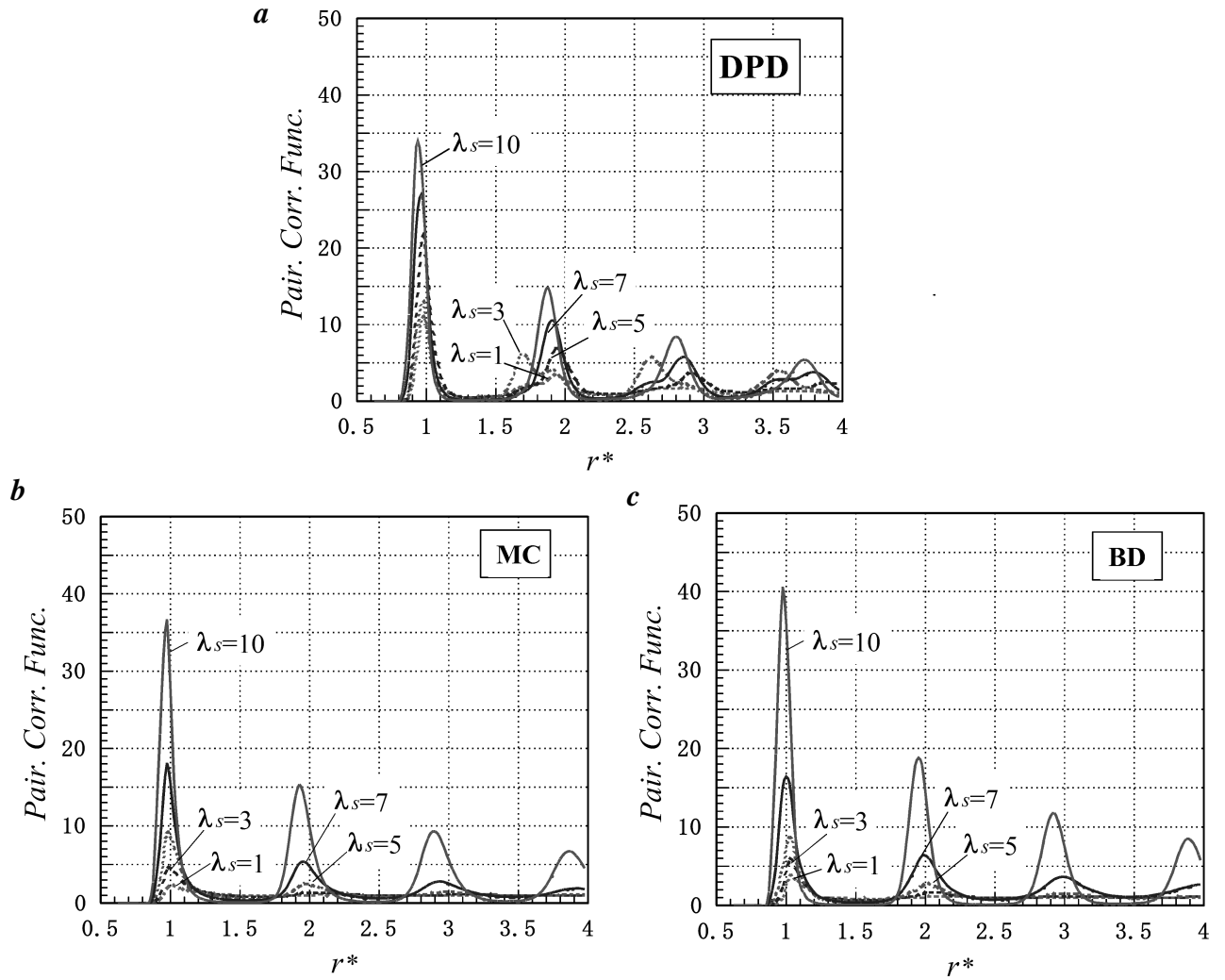


FIG.9. Pair correlation functions for various cases of λ_s^* : (a) for dissipative particle dynamics simulations; (b) for Monte Carlo simulations; (c) for Brownian dynamics simulations.

reasonable that the results for the case of $d_c^*=0.4$ and $m_d^*=0.01$ should be compared with those aggregate structures, since the cluster formation for this case is regarded as the physically most reasonable results from the above-mentioned discussion. For a quantitative comparison, the pair correlation function along the magnetic field direction is also shown in Fig. 9 for five cases of $\lambda_s=10, 7, 5, 3$ and 1.

It is seen that the present simulation results for $\lambda_s=10$, shown in Fig. 7(c), are in a qualitatively good agreement with those for Monte Carlo simulations in Fig. 8(a) and also with those for the Brownian dynamics simulations in Fig. 8(c). In addition, quantitative agreement is seen to be quite satisfactory from comparing the results for the pair correlation function, shown in Figs. 9(a), 9(b) and 9(c). However, if the snapshot for the case of $\lambda_s=3$, shown in Fig. 7(d), is compared with those obtained by other simulation methods, shown in Figs. 8(b) and 8(d), we see that the aggregate structures in Fig. 7(d) are significantly exaggerated. As already pointed out, this discrepancy shows again that the

present DPD simulation method with no rotational motion and the model potential is not applicable to the simulations of small interactions between magnetic particles such as $\lambda_s=3$. This becomes much clearer by comparing the results for the pair correlation function, shown in Fig. 9. That is, the results by the present DPD simulations for $\lambda_s=10$ agree well with those obtained by other simulation methods qualitatively and quantitatively, but the present aggregate structures come to exhibit a more significant correlation, compared with those of other simulations, as the value of λ_s decreases; in other words, more significant aggregates are formed. For comparison, the results obtained by Stokesian dynamics simulations are shown in Figs. 8(e) and 8(f). Since the Stokesian dynamics method does not take into account the particle Brownian motion, the aggregate structures are much more tight or compact than the other simulation results.

5. CONCLUSIONS

We have investigated the validity of the application of the dissipative particle dynamics (DPD) method to ferromagnetic colloidal dispersions by conducting DPD simulations for a two-dimensional system. The present simulation results have clearly shown that DPD simulations with the model interaction potential presented here give rise to physically reasonable aggregate structures under circumstances of strong magnetic particle-particle interactions as well as a strong external magnetic field, since these aggregate structures are in good agreement with those of Monte Carlo and Brownian dynamics simulations. Also, in order to activate the Brownian motion of magnetic particles, dissipative particles are not necessarily taken sufficiently small. This may be regarded as an important merit from a simulation point of view, since one can simulate physical phenomena for a smaller system with relatively short computation time. For advancing the present work, we need to develop, in future, another interaction model for magnetic and dissipative particles, which induces the particle rotational motion, and also need to combine the equation of the rotational motion in the present kinetic equations.

REFERENCES

1. Rothman, D. H., and Zaleski, S., "Lattice-Gas Cellular Automata," Cambridge Univ. Press, Cambridge, 1998.
2. Succi, S., "The Lattice Boltzmann Equation," Clarendon Press, Oxford, 2001.
3. Hoogerbrugge, P. J., and Koelman, J. M. V. A., *Europhys. Lett.* **19**, 155 (1992).
4. Koelman, J. M.V. A., and Hoogerbrugge, P. J., *Europhys. Lett.* **21**, 263 (1993).
5. Espanol, P., and Warren, P., *Europhys. Lett.* **30**, 191 (1995).
6. Espanol, P., *Phys. Rev. E* **52**, 1734 (1995).
7. Marsh, C. A., Backx, G., and Ernst, M. H., *Phys. Rev. E* **56**, 1676 (1997).
8. Satoh, A., and Majima, T., *J. Colloid Inter. Sci.* **283**, 251 (2005).
9. Allen, M. P., and Tildesley, D. J., "Computer Simulation of Liquids," Clarendon Press, Oxford, 1987.
10. Kamiyama, S., and Satoh, A., "Molecular Dynamics Simulations," Asakura Shoten, Tokyo,

1997. (in Japanese)

11. Satoh, A., "Introduction to Molecular-Microsimulation of Colloidal Dispersions," Elsevier Science, Amsterdam, 2003.
12. von Gottberg, F. K., Smith, K. A., and Hatton, T. A., *J. Chem Phys.* **106**, 9850 (1997).
13. Branka, A. C., and Heyes, D. M., *J. Chem. Phys.* **109**, 312 (1998).
14. Kirchhoff, Th., Lowen, H., and Klein, R., *Phys. Rev. E* **53**, 5011 (1996).
15. Choi, H. G., and Joseph, D. D., University of Minesota Supercomputing Institute Research Report, UMSI 2000/17, February 2000.
16. Glowinski, R., Pan, T. W., Hela, T. I., Joseph, D. D., and Piaux, J. A., University of Minesota Supercomputing Institute Research Report, UMSI 2000/68, April 2000.
17. Diaz-Goano, C., Mineev, P. D., and Nandakumar, K., *J. Comp. Phys.* **192**, 105 (2003).
18. Nguyen, N., -Q., and Ladd, A. J. C., *Phys. Rev. E.* **66**, 046708 (2002).
19. Boek, E. S., Coveney, P. V., Lekkerkerker, H. N. W., and P. van Schoot, *Phys. Rev. E.* **55**, 3124 (1997).
20. Satoh, A., *J. Colloid Inter. Sci.* **234**, 425 (2001).
21. Aoshima. M., and Satoh, A., *J. Colloid Inter. Sci.* **253**, 455 (2002).
22. Satoh, A., *J. Colloid Inter. Sci.* **262**, 263 (2003).
23. Aoshima, M., and Satoh, A., *J. Colloid Inter. Sci.* **280**, 83 (2004).
24. Satoh, A., *J. Colloid Inter. Sci.* **289**, 276 (2005).
25. Satoh, A., Ozaki, M., Ishikawa, T., and Majima, T., *J. Colloid Inter. Sci.* **292**, 581 (2005).
26. Satoh, A., Chantrell, R.W., Kamiyama, S., and Coverdale, G.N., *J. Colloid Inter. Sci.* **178**, 620 (1996).
27. Satoh, A., Chantrell, R.W., and Coverdale, G.N., *J. Colloid Inter. Sci.* **209**, 44 (1999).
28. Satoh, A., and Coverdale, G. N., *J. Colloid Inter. Sci.* **231**, 238 (2000).